2022-09

Embrittlement failure of 51CrV4 leaf springs

James, MN

10.1016/j.engfailanal.2022.106517
Engineering Failure Analysis
Elsevier BV

Engineering Failure Analysis 139 (2022) 106517

Contents lists available at ScienceDirect

Engineering Failure Analysis

journal homepage: www.elsevier.com/locate/engfailanal

Embrittlement failure of 51CrV4 leaf springs

M.N. James [a,b,*], D.G. Hattingh [b], L. Matthews [b]

[a] School of Engineering, Computing & Mathematics, University of Plymouth, Plymouth, England
[b] eNtsa, Nelson Mandela University, Port Elizabeth, South Africa

ARTICLE INFO

Keywords:
Leaf spring
51CrV4 steel
Environmental embrittlement
Pitting corrosion
Chloride cleaning

ABSTRACT

High strength quenched and tempered alloys are used in the manufacture of leaf springs, and peening techniques are used to induce compressive residual stresses on the tension surface of the individual leaves to resist fatigue crack growth. However, the extent of such residual stresses is usually limited to around 0.1–0.2 mm deep. Their beneficial effect can therefore be negated by corrosion pitting, while high strength steels are known to also be susceptible to environmental embrittlement in high chloride environments. This case study deals with an interesting example of environmental embrittlement of multileaf springs reportedly made from 60Si2Mn steel, but actually manufactured from 51CrV4 steel. Multiple cracks initiated from corrosion pits and fatigue failures occurred within 6–9 months from service entry of the vehicles. The embrittlement was triggered by the disinfecting and cleaning regime that reflected the use of the trucks for conveying animal feed.

1. Introduction

Leaf springs, originally called laminated or carriage springs, have been utilised in vehicles since the mid-17th century and their design is well understood in both metallic alloys [1,2] and composite materials [3,4]. The arduous fatigue and corrosion operating environment of metallic leaf springs necessitates the use of high strength quenched and tempered alloys (typically around 0.5% – 0.6 %C with Si, Mn, Cr, Mo, and V additions), e.g. 51CrV4, AISI 5160 and EN 45A. Care has to be taken in heat treatment to avoid decarburisation of the surface, and a peening process is generally applied on the tension side of the individual leaves to increase fatigue resistance by generating surface compressive stresses [5,6]. As noted in the work by Fragoudakis et al [6], the different steps in spring manufacture are designed to alter the microstructure of the steel to tempered martensite and to produce compressive residual stresses on the tension side through surface treatments. These both have a beneficial effect on the fatigue life of the leaf spring. There are a number of variants of peening techniques that have been applied to leaf springs, including laser peening [7] and stress peening, where a tensile stress is applied during the shot peening process, which leads to an increased compressive stress in the surface when the preload is released [8].

However, the beneficial influence of compressive residual stresses is confined to a relatively small layer on the surface of the individual spring leaves and, if the spring operates in a corrosive environment, pitting corrosion can occur leading to the early initiation of fatigue cracks. Shi et al [9] discussed the corrosion mechanism in spring steel and noted that small changes in the alloy composition could have a beneficial effect on the corrosion resistance, citing the addition of small amounts of B, V and Nb. It has also been reported that crack initiation in spring steel is influenced by the size, type, composition and distribution of inclusions [10,11]. Shi et al [9]

* Corresponding author.
E-mail address: mjames@plymouth.ac.uk (M.N. James).

https://doi.org/10.1016/j.engfailanal.2022.106517
Received 12 April 2022; Received in revised form 16 May 2022; Accepted 2 June 2022
Available online 6 June 2022
1350-6307/

Fig. 1. The failures occurred in the second master leaf, equally distributed on either the left or right side leaf springs, with the fractures occurring either ahead of the axle (40%) or behind it (60%).

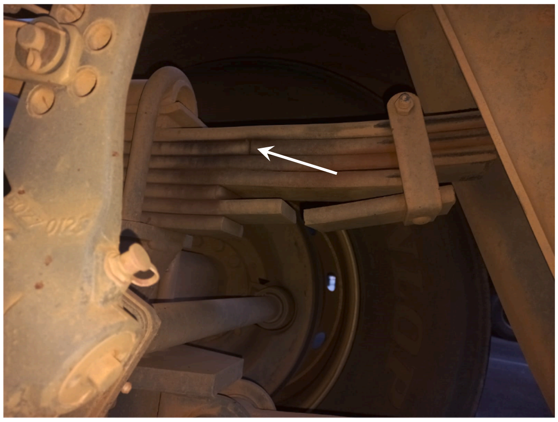

Fig. 2. In this spring assembly the first fracture in the second master leaf (arrow) has weakened the springs so that plastic deformation has occurred in the third and fourth leaves, and this has caused fracture in the fifth leaf.

further state that the pits form as the oxide or nitride inclusions are corroded and that this leads to hydrogen absorption and environmental embrittlement. Shibaeva et al [12] report that (Ca, Mg, Mn)S and SiO_2 inclusions all affect the local corrosion resistance of carbon steels, with those that contain Ca and S the most readily attacked by corrosion.

This paper reports a case study of failure in 7 layer multileaf springs, designed for an 8 tonne axle load and fitted to trucks, where pitting corrosion and environmental embrittlement have led to early fatigue failure in a number of vehicles. The primary cause of the failures was corrosion pitting penetrating through the shot peened surface layer, leading to multiple fatigue crack initiation sites with an environmental embrittlement component acting on the subsequent crack growth. It should be noted, however, that there are many sources of fatigue loading acting on the spring, including high frequency road vibration. Springs are protected against fatigue loading by shot peening on the tension surface to induce a plastically deformed layer, typically around 0.1–0.2 mm deep [13], where there is a high level of compressive residual stress. If corrosion pitting occurs on this surface, these local stress concentrations penetrate below the shot peened layer and rapid fatigue crack initiation occurs, as there is a counterbalancing zone of tensile stress below the compressive surface layer that detrimentally influences crack initiation and growth. In the presence case, there was an added component of embrittlement that is clearly observed in the fracture surface morphology.

Although several papers have been published that deal with failures in leaf springs, e.g. [14–16], it appears that no papers dealing with environmental embrittlement (EE) of leaf springs are available in the published literature. Equally, this case study highlights the importance of obtaining information relevant to the failure that may be seen as initially irrelevant by the client, but which is crucial to correctly identifying the cause of the problem and specifying a solution to avoid future failures.

2. The failed springs

The failed leaf springs are shown in Figs. 1 and 2 and the master leaf terminates in concave ends. Each leaf is 16 mm × 75 mm in cross-section. Failure were experienced some 6–9 months after the trucks entered service and invariably occurred initially in the

Fig. 3. The three fractured leaf springs delivered for investigation. The two halves are taped together in each case and are shown with the tension side up.

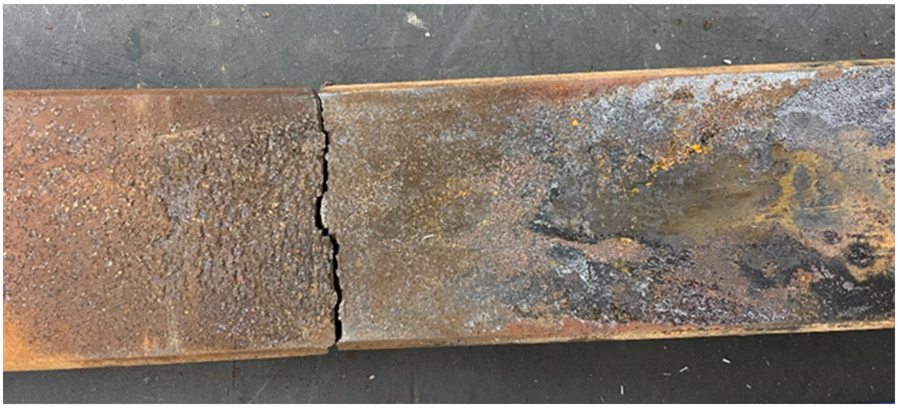

Fig. 4a. There is a significant amount of corrosion present on the tension surface of the fractured leaves, and the fracture surfaces are unusually jagged for a fatigue fracture.

second master leaf (Fig. 1), with consequent plastic deformation in the lower leaves sometimes causing failure to occur in the fifth leaf (Fig. 2). The vehicle manufacturer reported that all the failed springs were on trucks operated by a single client and that the trucks were used to deliver animal feed.

Three fractured leaves were delivered for investigation into the cause of the failures (Fig. 3. and 4) and the fracture surfaces were all heavily corroded, as seen in Fig. 5. Fig. 4a shows that a significant level of corrosion is present on the tension surface of the fractured leaves and, in addition, the fracture surfaces are unusually jagged for a fatigue fracture Fig. 4b). The import of these observations will become clear in sections 3 and 4 of the paper. A typical set of fracture surfaces are seen in Fig. 5 which shows the one chosen for fractographic analysis, and Fig. 6 shows this fracture surface after ultrasonic derusting in dilute nitric acid (a 2% Nital solution made up as 3.6 ml of 55% Nitric acid in 100 ml of distilled water). Any additional corrosion introduced during this cleaning process would be minor compared with its initial state.

It is clear in Fig. 6 that there is a network of cracks on the fracture surface and this was proven to be the case using scanning electron microscopy (Fig. 7). The failure mechanism is clearly fatigue and there are several initiation sites on the tension side of the leaf spring, with the main one indicated with the black arrow in Fig. 6. This observation, together with the colony of surface cracks seen in Figure 4 indicate that some form of embrittlement has occurred.

These leaf springs were stated to have been manufactured from 60Si2Mn steel, which is equivalent to DIN 1.0909 and Table 1 gives the specification for this alloy, the chemical composition supplied by the manufacturer of the steel, along with the results from analysis of the springs. The chemical analysis of the spring samples was done using a Bruker Q4 Tasman spectrometer. It is clear that the chemical analysis of the failed spring conforms better with the 51CrV4 steel specification (EN 10083–3:2006). This change in steel grade is not expected to have been a significant influence on the failure, as 51CrV4 steel has very similar mechanical properties to the 60Si2Mn steel. The tensile data supplied by the manufacturer gives the yield strength as $\sim$ 1200 MPa with a tensile strength of $>$ 1300

Fig. 4b. A colony of surface cracks can be seen on the tension surface, running parallel with the fracture surface. The image shows two different fracture surfaces and the one on the right has been derusted in dilute nitric acid.

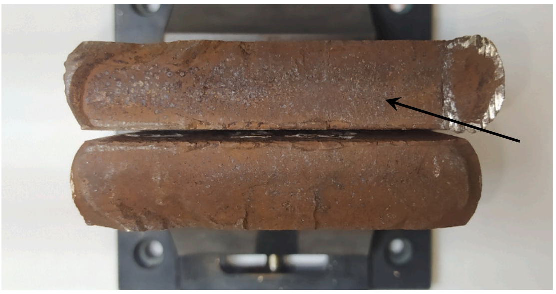

Fig. 5. As-received fracture surfaces from the fractured spring that was chosen for a detailed fractographic and metallographic investigation. The arrow indicates the surface that was chosen for detailed fractography.

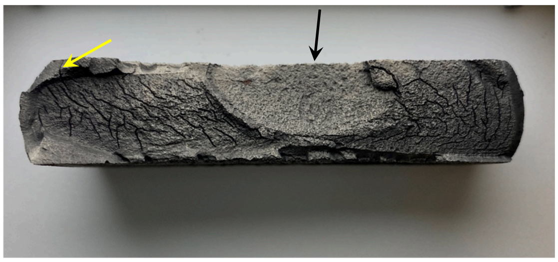

Fig. 6. After cleaning, a network of cracks can be seen on the fracture surface and these were proven to be cracks using scanning electron microscopy. The failure mechanism is clearly fatigue and there are several initiation sites, with the main one indicated with the black arrow.

MPa in the quenched and tempered condition, and a Rockwell C hardness value of around 43 (equivalent to a Vickers diamond hardness of $H_V \approx 430$). These hardness and strength values could change significantly depending on the actual heat treatment cycle used for the leaf springs. The leaves were further stated to have been shot blasted on the tensile (concave) side.

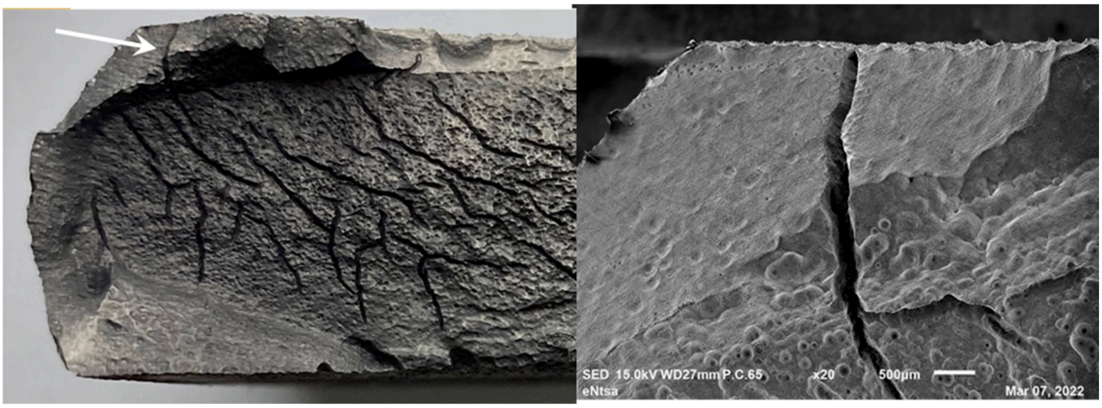

Fig. 7. This SEM image shows that the dark lines are, in fact, cracks and the crack shown is marked with the yellow arrow in Fig. 6. (For interpretation of the references to colour in this figure legend, the reader is referred to the web version of this article.)

Table 1
Chemical composition of the leaf spring steel.

	C(wt%)	Mn(wt%)	Si(wt%)	P(wt%)	S(wt%)	Cr(wt%)	V(wt%)	Ni(wt%)	Cu(wt%)
60Si2Mn [1]	0.56–0.64	0.60–0.90	1.50–2.00	≤0.035	≤0.035	0.35 max	–	0.35 max	–
51CrV4 [2]	0.47–0.55	0.70–1.10	0.40max	0.025max	0.025max	0.90–1.20	0.10–0.25	<0.01	
Mill	0.59	0.79	1.60	0.024	0.008	0.09	–	0.03	0.04
Specimens	0.53	0.72	0.24	0.013	<0.005	1.03	0.15	0.01	<0.01

[1] According to Chinese National standard GB1222-84
[2] According to Euronorm standard EN 10083–3: 2006

Fig. 8. Metallographic sections were cut perpendicular to the fracture surface (marked as 1), to sample the colony of surface cracks, and parallel with the fracture surface (marked as 2).

3. Metallography

Specimens were cut from a second failed spring for metallography and hardness testing and Fig. 8 shows the orientation of the metallographic specimens, with the specimen marked 1 cut perpendicular to the fracture surface and specimen 2 being parallel with the fracture surface. Polishing followed the standard route, finishing with 6 µm diamond paste and etching used a 2% Nital solution made up as 3.6 ml of 55% Nitric acid in 100 ml of distilled water. Microstructures were imaged using an Olympus DSX510 digital microscope with Olympus Stream software. Fig. 9 gives the polished and macro-etched section of specimen 1 which shows the severe surface pitting corrosion in the region adjacent to the fracture, and a series of cracks which decline in size with distance from the fracture surface. The reduction in size reflects the decline in the applied stress away from the plane of maximum bending stress in the

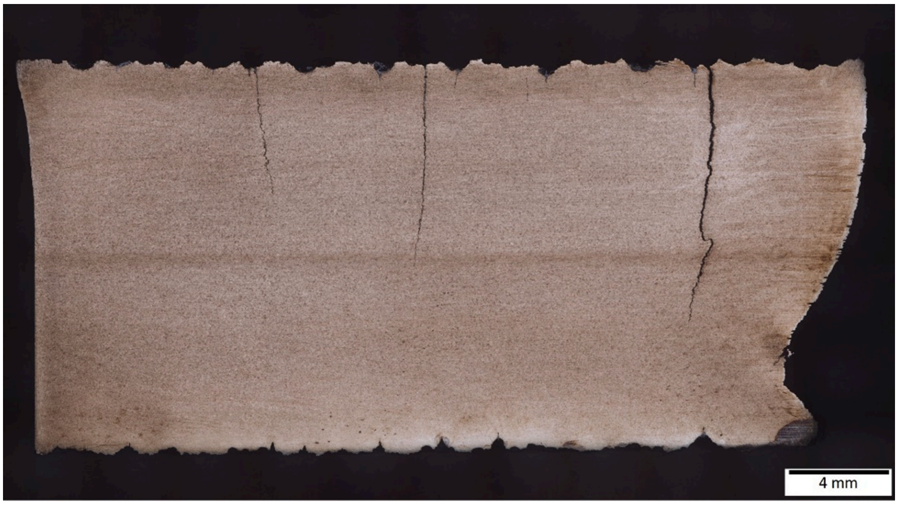

Fig. 9. This macro-etched section in the plane of specimen 1 shows the severe surface pitting corrosion in the region adjacent to the fracture, and a series of cracks which decline in size with distance from the fracture surface. Cracks have initiated at virtually every corrosion pit in this region.

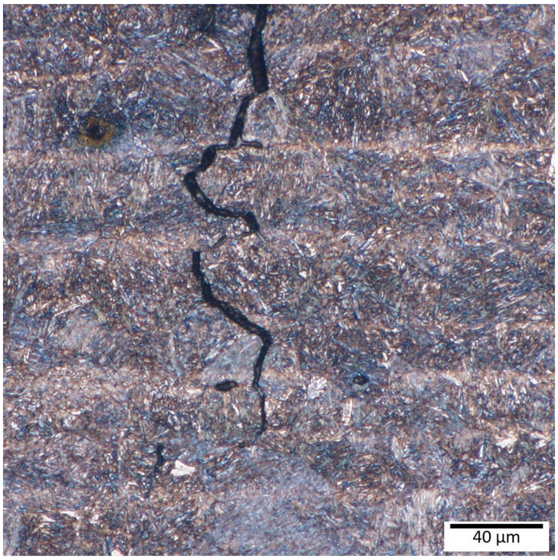

Fig. 10. Examination at higher magnification reveals the expected quenched and tempered martensitic microstructure, demonstrate that the cracks are intergranularand branched and may not extend to the surface, at least in this plane. 305x magnification.

second master leaf, which is where the fracture has occurred.

Examination at higher magnification demonstrated that the springs had the expected quenched and tempered martensitic microstructure, and also showed that the cracks were intergranular and branched and did not extend to the surface in all cases, at least in the plane of the metallographic section (Fig. 10). In addition, almost every corrosion pit had a small crack initiated from it, as illustrated in Fig. 11. The intergranular, branched and discontinuous nature of the cracks provides further evidence that embrittlement of the steel has occurred. Microhardness values were measured using a Vickers diamond indenter under a 500 gf load both perpendicular to, and parallel with, the fracture surface, giving an overall average value of 440 H_V with a variation between 430 and 445 H_V. This is in line with the alloy's datasheet and indicates that the heat treatment of the steel had been correctly performed. Inappropriate heat treatment procedures are known to lead to premature spring failure, either because of improper quenching [17] or from surface decarburization which lowers the tensile and fatigue strength of the alloy and can lead to premature spring failure [18]. No evidence of any near-surface decarburization was observed (Fig. 12).

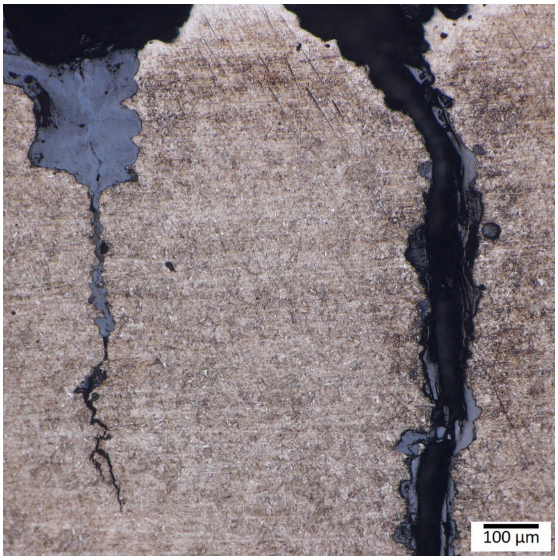

Fig. 11. Cracks have initiated from corrosion pits and have oxide extending significant distances down them. 277x magnification.

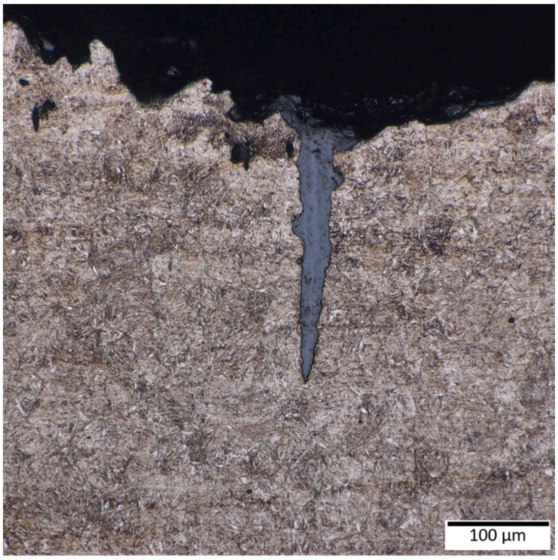

Fig. 12. No evidence of any surface decarburization was seen and the microstructure is clearly tempered martensite in this image at 500x magnification.

4. Environmental embrittlement

During the metallographic examination, a number of near-surface inclusion clusters were observed and several of the inclusions were examined using energy dispersive analysis of X-rays (EDAX) in a JEOL JSM-IT200 scanning electron microscope fitted with a ThermoFisher Noran System 7. This showed that some of the inclusions had high levels of Ca and S, while others contained high levels of Ti and V, and examples of the chemical analysis are given in Figs. 13a and 13b. Work by Shi et al [19] on the effect of nonmetallic inclusions on localised inclusions in 60Si2Mn spring steel has demonstrated that severe localised corrosion occurred in areas of clustered CaS inclusions and that CaS inclusions were the main source of environmental embrittlement in a chloride environment. They also observed that clustered CaS inclusion areas triggered a corrosion tunnel effect, causing corrosion pits to form, even below the metal surface. Komazaki et al [20] investigated the environmental embrittlement of six different 0.50 %C spring steels in wet-dry cyclic corrosion tests in a 5mass% NaCl solution, and concluded that the susceptibility to EE increases with tensile strength and is closely associated with a decreased resistance to pitting corrosion. The overall conclusion from these two studies is that 60Si2Mn spring steel is susceptible to environmental embrittlement in a wet-dry cyclic chloride environment, and it would be expected that 51CrV4 would

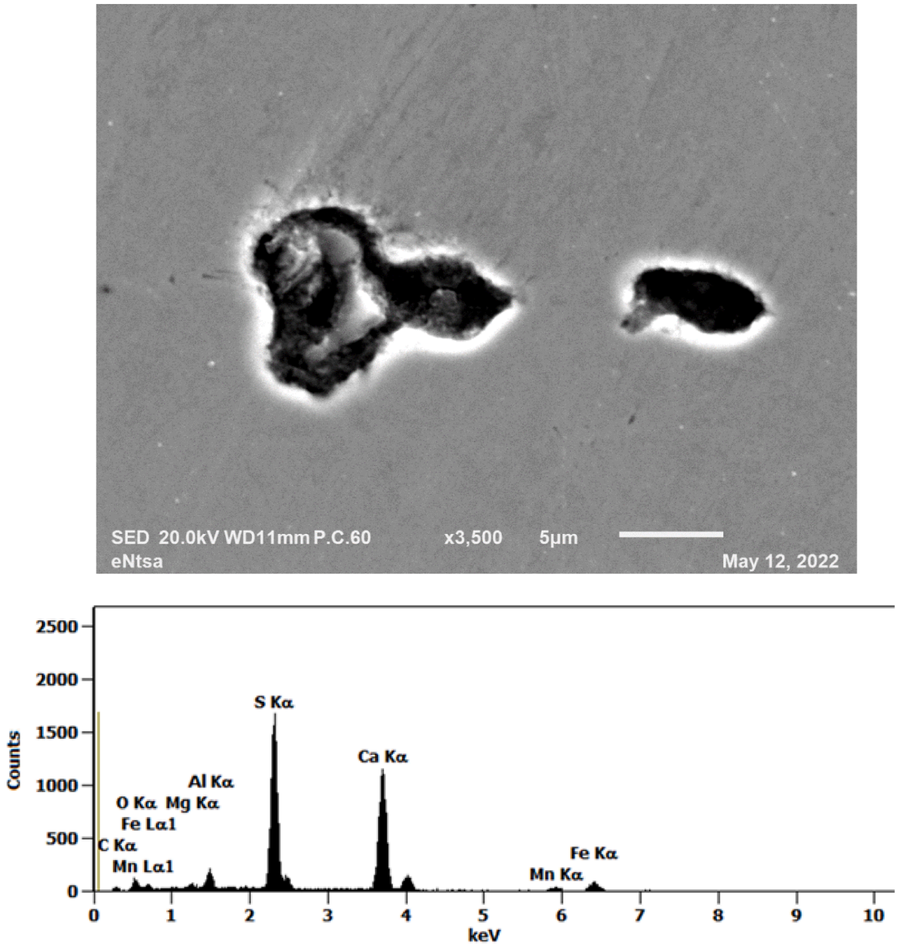

Wt%	C	O	Mg	Al	S	Ca	Mn	Fe
inclusion(4)_pt1	3.1	5.4	0.5	2.6	29.9	42.7	4.7	10.9

Fig. 13a. Typical high Ca and high S spectrum observed on a number of small inclusions in the 51CrV4 steel.

show similar corrosion behaviour.

At this point, the origin of the chloride-containing environment was not clear, but in a conversation with the truck manufacturer, it transpired that a corrosion problem with electrical circuits on these trucks had been experienced previously, as the trucks were regularly disinfected. Samples of the cleaning water had been sent for analysis, and this had revealed that the water used to clean the vehicles was acidic (pH $\sim$ 4.6–5.1) and highly corrosive with a Langelier saturation index between -3.72 and -4.7 (severe corrosion), with high levels of dissolved chlorides (549–594 mg/l).

5. Conclusions

The disinfecting and cleaning regime employed by the truck operator has led to wet-dry corrosion cycles with an additional contribution from the oxygen concentration cell forming in the slight gap between the master and second master leaves, as evidenced by the severe pitting and associated cracking seen in this region. Severe pitting has been assisted by the clustered CaS-type inclusions in the 51CrV4 steel alloy and this has led to hydrogen-induced environmental embrittlement from the high chloride ion cleaning solution. Multiple intergranular cracks have been initiated by EE, that could then easily extend under the applied cyclic fatigue loading (Figures 4 and 9). Once the semi-elliptic fatigue crack was around 13 mm deep the second master spring fractured under the applied loading which overloaded the third and fourth leaves, leading to plastic deformation. This increased the loading in the fifth leaf, sometimes leading to a second fracture in the leaf spring assembly.

It was recommended that the truck manufacturer liaise with the operator to see whether a less corrosive cleaning/disinfecting regime could be implemented.

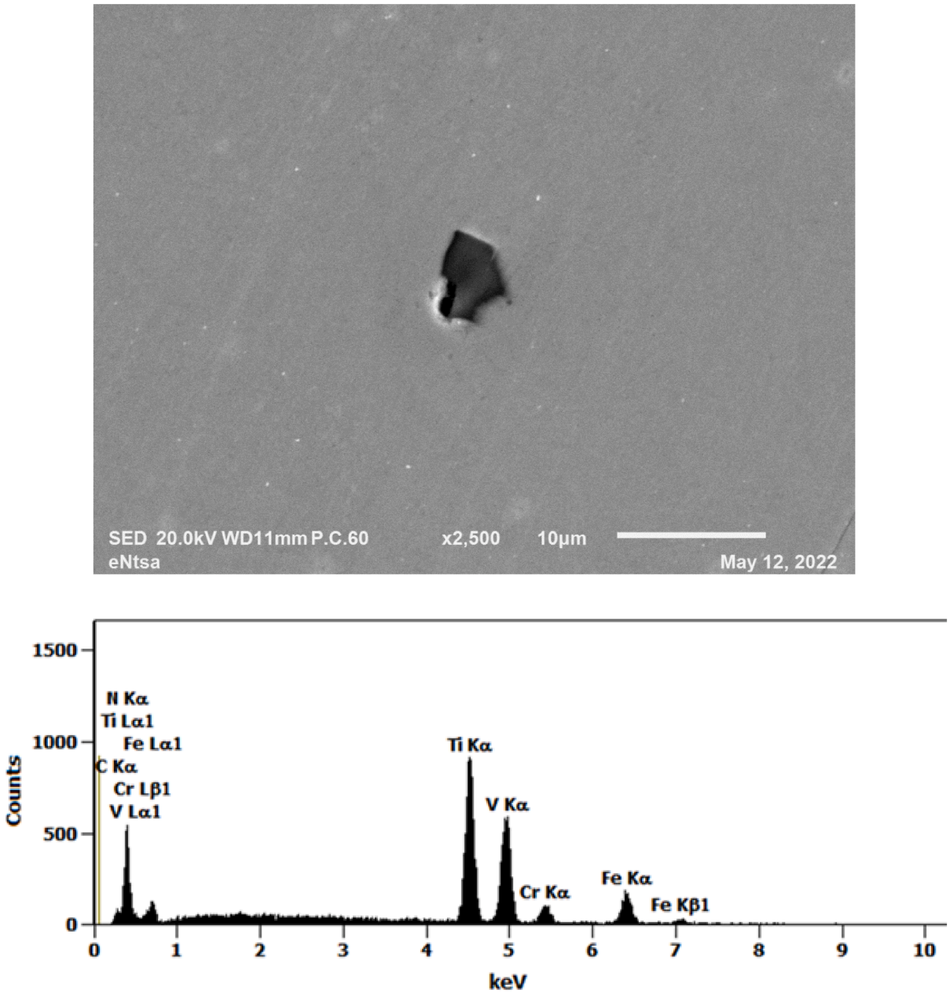

Wt%	C	N	Ti	V	Cr	Fe
inclusion(2)_pt1	1.7	12.9	38.8	27.3	1.9	17.4

Fig. 13b. Typical high Ti and high V spectrum observed on some small inclusions in the 51CrV4 steel.

Declaration of Competing Interest

The authors declare that they have no known competing financial interests or personal relationships that could have appeared to influence the work reported in this paper.

References

[1] K. Kumar, M.L. Aggarwal, Optimization of Various Design Parameters for EN45A Flat Leaf Spring, Mater. Today:. Proc. 4 (2017) 1829–1836.
[2] M. Bakir, B. Ozmen, C. Donertas, Correlation of Simulation, Test Bench and Rough Road Testing in terms of Strength and Fatigue Life of a Leaf Spring, Procedia Eng. 213 (2018) 303–312.
[3] J. Ke, Z.-Y. Wu, X.-Y. Chen, Z.-P. Ying, A review on material selection, design method and performance investigation of composite leaf springs, Compos. Struct. 226 (2019), 111277.
[4] K. Ashwini, C.V. Mohan Rao, Design and Analysis of Leaf Spring using Various Composites – An Overview, Mater. Today:. Proc. 5 (2018) 5716–5721.
[5] A. Kubit, M. Bucior, W. Zielecki, F. Stachowicz, The impact of heat treatment and shot peening on the fatigue strength of 51CrV4 steel, Procedia Struct. Integrity 2 (2016) 3330–3336.
[6] R. Fragoudakis, G. Savaidis, N. Michailidis, Optimizing the development and manufacturing of 56SiCr7 leaf springs, Int. J. Fatigue 103 (2017) 168–175.
[7] P. Ganesh, R. Sundar, H. Kumar, R. Kaul, K. Ranganathan, P. Hedaoo, et al., Studies on laser peening of spring steel for automotive applications, Opt. Lasers Eng. 50 (2012) 678–686.
[8] Q. Feng, C. Jiang, Z. Xu, Surface layer investigation of duplex stainless steel S32205 after stress peening utilizing X-ray diffraction, Mater. Des. 47 (2013) 68–73.
[9] W. Shi, S. Yang, A. Dong, J. Li, Understanding the Corrosion Mechanism of Spring Steel Induced by MnS Inclusions with Different Sizes, JOM. 70 (2018) 2513–2522.
[10] Y. Furuya, T. Abe, Effect of mean stress on fatigue properties of 1800MPa-class spring steels, Mater. Des. 32 (2011) 1101–1107.

[11] H. Mayer, R. Schuller, U. Karr, M. Fitzka, D. Irrasch, M. Hahn, et al., Mean stress sensitivity and crack initiation mechanisms of spring steel for torsional and axial VHCF loading, Int. J. Fatigue 93 (2016) 309–317.
[12] T.V. Shibaeva, V.K. Laurinavichyute, G.A. Tsirlina, A.M. Arsenkin, K.V. Grigorovich, The effect of microstructure and non-metallic inclusions on corrosion behavior of low carbon steel in chloride containing solutions, Corros. Sci. 80 (2014) 299–308.
[13] W. Koenecke, N.K. Burrell, C. Mehelich, Shot peening springs, Springs. (1982) 7.
[14] C.K. Clarke, G.E. Borowski, Evaluation of a Leaf Spring Failure, J. Fail. Anal. Prev. 5 (6) (2005) 54–63.
[15] J.J. Fuentes, H.J. Aguilar, J.A. Rodríguez, E.J. Herrera, Premature fracture in automobile leaf springs, Eng. Fail. Anal. 16 (2009) 648–655.
[16] Husaini, R.H. Liza, A. Nurdin, S. Muammar, Failure analysis of a fractured leaf spring as the suspension system applied on the dump truck, in: A.a.M. Iqbal (Ed.), Second International Conference on Experimental and Computational Mechanics in Engineering, Trans Tech Publications, Indonesia, 2020.
[17] N.K. Mukhopadhyay, S.K. Das, B. Ravikumar, V.R. Ranganath, S. Ghosh Chowdhury, Premature failure of a leaf spring due to improper materials processing, Eng. Fail. Anal. 4 (1997) 161–170.
[18] J.M.A.M. Rocha, A.R. Pimenta, S.R. Correa, M. Cindra Fonseca, M.G. Diniz, Fracture failure analysis in compression spring of a wagon torpedo, Eng. Fail. Anal. 122 (2021), 105245.
[19] W.-N. Shi, S.-F. Yang, J.-S. Li, Effect of nonmetallic inclusions on localized corrosion of spring steel, Int. J. Miner. Metall. Mater. 28 (3) (2021) 390–397.
[20] S.-I. Komazaki, K. Kobayashi, T. Misawa, T. Fukuzumi, Environmental embrittlement of automobile spring steels caused by wet–dry cyclic corrosion in sodium chloride solution, Corros. Sci. 47 (2005) 2450–2460.